THE JOURNAL OF BIOLOGICAL CHEMISTRY VOL. 281, NO. 42, pp. 31419–31429, October 20, 2006

Extracellular NAD^+ Is an Agonist of the Human $P2Y_{11}$ Purinergic Receptor in Human Granulocytes*

Received for publication, July 12, 2006, and in revised form, August 9, 2006 Published, JBC Papers in Press, August 22, 2006, DOI 10.1074/jbc.M606625200

Iliana Moreschi[‡], Santina Bruzzone[‡1], Robert A. Nicholas[§], Floriana Fruscione[‡], Laura Sturla[‡], Federica Benvenuto[¶], Cesare Usai[‖], Sabine Meis[**], Matthias U. Kassack[**], Elena Zocchi[‡], and Antonio De Flora[‡]

*From the [‡]Department of Experimental Medicine, Section of Biochemistry, and Center of Excellence for Biomedical Research (CEBR), University of Genova, Viale Benedetto XV/1, 16132 Genova, Italy, the [§]Department of Pharmacology, University of North Carolina, Chapel Hill, North Carolina 27599-7365, the [¶]Neuroimmunology Unit, Department of Neurosciences, Ophthalmology and Genetics, and CEBR, University of Genova, Genova, Italy, the [‖]Institute of Biophysics, National Research Council, Via De Marini 6, 16149 Genova, Italy, and the **Pharmaceutical Institute, University of Bonn, An der Immenburg 4, Bonn D-53121, Germany*

Micromolar concentrations of extracellular β-NAD^+ (NAD_e^+) activate human granulocytes (superoxide and NO generation and chemotaxis) by triggering: (i) overproduction of cAMP, (ii) activation of protein kinase A, (iii) stimulation of ADP-ribosyl cyclase and overproduction of cyclic ADP-ribose (cADPR), a universal Ca^{2+} mobilizer, and (iv) influx of extracellular Ca^{2+}. Here we demonstrate that exposure of granulocytes to millimolar rather than to micromolar NAD_e^+ generates both inositol 1,4,5-trisphosphate (IP_3) and cAMP, with a two-step elevation of intracellular calcium levels ($[Ca^{2+}]_i$): a rapid, IP_3-mediated Ca^{2+} release, followed by a sustained influx of extracellular Ca^{2+} mediated by cADPR. Suramin, an inhibitor of P2Y receptors, abrogated NAD_e^+-induced intracellular increases of IP_3, cAMP, cADPR, and $[Ca^{2+}]_i$, suggesting a role for a P2Y receptor coupled to both phospholipase C and adenylyl cyclase. The $P2Y_{11}$ receptor is the only known member of the P2Y receptor subfamily coupled to both phospholipase C and adenylyl cyclase. Therefore, we performed experiments on $hP2Y_{11}$-transfected 1321N1 astrocytoma cells: micromolar NAD_e^+ promoted a two-step elevation of the $[Ca^{2+}]_i$ due to the enhanced intracellular production of IP_3, cAMP, and cADPR in 1321N1-$hP2Y_{11}$ but not in untransfected 1321N1 cells. In human granulocytes NF157, a selective and potent inhibitor of $P2Y_{11}$, and the down-regulation of $P2Y_{11}$ expression by short interference RNA prevented NAD_e^+-induced intracellular increases of $[Ca^{2+}]_i$ and chemotaxis. These results demonstrate that β-NAD_e^+ is an agonist of the $P2Y_{11}$ purinoceptor and that $P2Y_{11}$ is the endogenous receptor in granulocytes mediating the sustained $[Ca^{2+}]_i$ increase responsible for their functional activation.

Extracellular NAD^+ (NAD_e^+)[2] is known to increase intracellular calcium concentrations ($[Ca^{2+}]_i$) in different cell types and by different mechanisms (1–8). In cells expressing the ecto-ADP-ribosyl cyclase (ADPRC) CD38, *e.g.* in CD38-transfected fibroblasts and HeLa cells, as well as in native astrocytes, retinal Muller cells and osteoblasts, direct conversion of NAD^+ to the Ca^{2+} mobilizer cyclic ADP-ribose (cADPR) (9) has been implicated as the principal mechanism leading to increases in $[Ca^{2+}]_i$ in response to NAD_e^+ (1, 3–6). In murine T lymphocytes, NAD_e^+ is the substrate of the ecto-enzyme mono-ADP-ribosyltransferase, which ADP-ribosylates the purinoceptor P2X7 or a P2X7-associated protein, leading to Ca^{2+} influx, formation of large pores, and cell death (7, 10, 11). In human monocytes, NAD_e^+ and ADPR trigger influx of extracellular Ca^{2+}, but neither CD38 nor P2X7-induced pore formation are involved (8).

Recently, we demonstrated that NAD_e^+ behaves as a pro-inflammatory cytokine targeting human polymorphonuclear granulocytes (12). Exposure of granulocytes to micromolar concentrations of NAD_e^+ (either the naturally occurring β or the α form) triggered the following cascade of causally related events: (i) activation of adenylyl cyclase and a rapid increase of intracellular cAMP levels, (ii) PKA-mediated stimulation of ADPRC activity and elevation of intracellular cADPR levels, and (iii) sustained $[Ca^{2+}]_i$ rise, due to influx of extracellular Ca^{2+} (12). Increases in $[Ca^{2+}]_i$ are known to be responsible for activation of human granulocytes (13). Indeed, NAD_e^+-induced $[Ca^{2+}]_i$ elevation triggered increased O_2^- and NO generation and enhanced chemotaxis toward NAD_e^+. Therefore, the results obtained with NAD_e^+-stimulated granulocytes (12) support a key role of cADPR in control of receptor-mediated chemotaxis in murine and human granulocytes, as previously demonstrated both *in vivo* (14) and *in vitro* (15).

The rapid increase of $[cAMP]_i$ in granulocytes that follows NAD_e^+ exposure (12) suggested that NAD_e^+ interacts with an

* This work was supported by grants from the Associazione Italiana per la Ricerca sul Cancro, the Italian Ministry of Education, University and Scientific Research (Grants MIUR-PRIN 2003, MIUR FIRB RBAUO19A3C, MIUR FIRB RBNE01ERXR, and MIUR FIRB RBLA039LSF), the University of Genova, and the Fondazione Cassa di Risparmio di Genova e Imperia. The costs of publication of this article were defrayed in part by the payment of page charges. This article must therefore be hereby marked "*advertisement*" in accordance with 18 U.S.C. Section 1734 solely to indicate this fact.

[1] To whom correspondence should be addressed: Dept. of Experimental Medicine, Section of Biochemistry, University of Genova, Viale Benedetto XV/1, 16132 Genova, Italy. Tel.: 39-010-353-8158; Fax: 39-010-354-415; E-mail: santina.bruzzone@unige.it.

[2] The abbreviations used are: NAD_e^+, extracellular NAD^+; $[Ca^{2+}]_i$, intracellular calcium concentration; ADPRC, ecto-ADP-ribosyl cyclase; cADPR, cyclic ADP-ribose; PCA, perchloric acid; ATP_e, extracellular ATP; IP_3, inositol 1,4,5-trisphosphate; $[cADPR]_i$, intracellular cADPR concentration; $[cAMP]_i$, intracellular cAMP concentration; AC, adenylate cyclase; PLC, phospholipase C; PKA, cAMP-activated protein kinase; siRNA, short interference RNA; CI, chemotaxis index; fMLP, formylmethionylleucylphenylalanine; HBSS, Hanks' balanced salt solution; GFP, green fluorescent protein; h2PY, human G protein-coupled P2Y receptor.

unidentified receptor, which activates the signaling cascade involving cADPR and increased $[Ca^{2+}]_i$ that eventually results in enhanced respiratory burst and chemotaxis. In the present study, we challenged granulocytes with millimolar NAD^+_e. Under these conditions, we observed a qualitatively different Ca^{2+} response, *i.e.* a biphasic one, with an initial inositol 1,4,5-trisphosphate (IP_3)-mediated peak of $[Ca^{2+}]_i$ caused by release from intracellular stores, followed by sustained influx of extracellular Ca^{2+}. Given that (i) NAD^+ is a nucleotide and (ii) NAD^+_e-induced intracellular increases of IP_3, cAMP, cADPR, and $[Ca^{2+}]_i$ were abrogated by suramin, a relatively non-selective inhibitor of P2Y receptors, we focused on the possibility that the signaling activities promoted by NAD^+_e were the result of activation of a G protein-coupled P2Y receptor. The signaling properties of P2Y receptors characterized to date suggested the $P2Y_{11}$ receptor as a putative NAD^+ receptor, because its activation increases both IP_3 and cAMP levels by virtue of its dual coupling to G_q and G_s (16–18). Results obtained with $hP2Y_{11}$-transfected 1321N1 astrocytoma cells reveal that β-NAD^+ is an agonist of the $P2Y_{11}$ purinoceptor. In addition, the use of NF157 (a recently synthesized, selective inhibitor of $P2Y_{11}$) and the down-regulation of $P2Y_{11}$ expression by short interfering RNA (siRNA) demonstrate that endogenous $P2Y_{11}$ is responsible for the NAD^+_e-induced activation of human granulocytes.

EXPERIMENTAL PROCEDURES

Materials—FLUO-3AM and FURA-2AM were obtained from Calbiochem (Milan, Italy). The [^{3}H]cAMP and [^{3}H]IP_3 assay systems and Ficoll-Paque Plus were purchased from Amersham Biosciences. A5 peptide (sequence: H_2N-SLLWLT-CRPWEAM-OH) was obtained from New England Peptide, Inc. (Gardner, MA). Dulbecco's modified Eagle's medium and RPMI cell culture medium were purchased from Cambrex Bio Science Milano (Bergamo, Italy). NF157 was synthesized as described (19). All other chemicals were obtained from Sigma (Milan, Italy).

High-performance Liquid Chromatography Analyses of Nucleotides and Chromatographic Purification of α- and β-NAD$^+$—High-performance liquid chromatography analyses of nucleotides and purification of α- and β-NAD^+ were performed as described previously (12).

Isolation of Human Granulocytes—Buffy coats, prepared from freshly drawn blood of healthy volunteers, were provided by Galliera Hospital, Genova, Italy. Granulocytes were isolated from the buffy coats as described before (12).

Cell Culture—Control and $hP2Y_{11}$-transfected 1321N1 astrocytoma cell lines (17) were cultured in Dulbecco's modified Eagle's medium supplemented with fetal calf serum (10%), penicillin (50 units/ml), and streptomycin (50 μg/ml) in a humidified 5% CO_2 atmosphere at 37 °C.

Fluorometric Measurements of $[Ca^{2+}]_i$—Freshly prepared granulocytes (10×10^6/ml) were loaded with 10 μM FLUO-3AM for 45 min at 25 °C in RPMI medium, washed with Hanks' balanced salt solution (HBSS, cat. no. H8264, Sigma), and resuspended in the same solution or in Ca^{2+}-free HBSS (cat. no. H6648, Sigma) at 5×10^6 cells/ml. $[Ca^{2+}]_i$ measurements were performed in 96-well plates (10^6 cells/well), and fluorescence (excitation, 485 nm; emission, 520 nm) was measured every 3 s with a fluorescence plate reader (Fluostar Optima, BMG Labtechnologies GmbH, Offenburg, Germany). The intensity of emitted light was plotted as a function of time. For $[Ca^{2+}]_i$ calibration, granulocytes were loaded with 10 μM FURA-2AM for 45 min at 25 °C in RPMI medium, and measurements were performed as described in a previous study (12).

Control and $hP2Y_{11}$-transfected 1321N1 cells were seeded in 96-well plates (2×10^4 cells/well). After 24 h, cells were loaded with 10 μM FLUO-3AM for 45 min at 25 °C in complete medium (Dulbecco's modified Eagle's medium) and washed once with 0.2 ml of HBSS. The indicated concentrations of nucleotides in HBSS (0.1 ml) were then added, and $[Ca^{2+}]_i$ measurements were performed using the fluorescence plate reader, as described above.

Determination of Intracellular cADPR Levels—Granulocytes (40×10^6/ml) were incubated for 0, 15, and 60 min at 25 °C in the absence (control) or in the presence of 1 mM α-NAD^+. At each time point, a 500-μl aliquot of the cell suspension was withdrawn and centrifuged at $5{,}000 \times g$ for 15 s, and the resulting cell pellets were lysed at 4 °C with 500 μl of 0.6 M perchloric acid (PCA). After centrifugation to remove precipitated proteins, the cADPR content was measured on the neutralized PCA cell extracts by a highly sensitive enzymatic cycling assay (20). cADPR levels were expressed as picomoles/10^6 cells.

Control and $hP2Y_{11}$-transfected 1321N1 cells were seeded in 35×10-mm dishes (2.4×10^5 cells/dish). After 48 h, the medium was removed and HBSS was added (0.6 ml). ATP or α-NAD^+ was added: the incubation was stopped after 15 min by removal of HBSS and addition of 300 μl if ice-cold PCA (0.6 M), and cells were removed by scraping. Cell extracts were centrifuged to remove precipitated proteins, and the cADPR content was measured on the neutralized cell extracts as described above.

Determination of Intracellular cAMP Levels—Granulocytes were suspended in HBSS or in Ca^{2+}-free HBSS (30×10^6/ml), preincubated for 5 min at 25 °C in the presence of the cAMP phosphodiesterase inhibitor 4-(3-butoxy-4-methoxybenzyl)imidazolidin-2-one (Ro 20-1724, Sigma, cat. no. B8279) (10 μM), and then challenged with vehicle or 1 mM α- or β-NAD^+. At different times (0, 20, 40, 60, 150, and 300 s), a 300-μl aliquot of the suspension was withdrawn, and the reaction was stopped by adding 20 μl of 9 M PCA at 4 °C. PCA was removed as described (20). Intracellular cAMP levels (expressed as picomoles of cAMP/10^6 cells) were determined by radioimmunoassay according to the manufacturer's protocol.

Control and $hP2Y_{11}$-transfected 1321N1 cells were seeded in 35×10 mm dishes (5×10^5 cells/dish). After 24 h, the medium was removed and HBSS was added (0.6 ml). Cells were then challenged with ATP or α- or β-NAD^+, and at different times the incubation mixtures were stopped by removal of HBSS and addition of 200 μl of ice-cold PCA (0.6 M). Cells were removed by scraping, the cell extracts were centrifuged to remove the proteins, and the cAMP levels in the neutralized cell extracts were measured as described above.

Determination of Intracellular IP_3 Levels—Granulocytes were resuspended in HBSS (40×10^6/ml) and challenged with 1 mM β-NAD^+. Aliquots of the suspensions (500 μl) were with-

drawn at different times (0, 30, and 90 s), and the reaction was stopped by adding 30 μl of 9 M PCA at 4 °C. Following removal of PCA (20), intracellular IP_3 levels were determined by radioimmunoassay. Results were expressed as picomoles of $IP_3/10^6$ cells.

Control and $hP2Y_{11}$-transfected 1321N1 cells were seeded in 35 × 10-mm dishes (5×10^5 cells/dish). After 24 h, the medium was removed and HBSS was added (0.6 ml). Cells were challenged with ATP or α- or β-NAD^+, and at various times (0, 30, 90, and 900 s) HBSS was removed and 300 μl of ice-cold PCA (0.6 M) was added. The cells were scraped, the precipitated proteins were removed by centrifugation, and IP_3 levels were measured on the supernatants of the neutralized cell extracts as described above.

Assays of ADP-ribosyl Cyclase Activity—$hP2Y_{11}$-transfected 1321N1 cells (4×10^6/ml) were incubated at 25 °C in the absence (control) or in the presence of 0.1 mM α-NAD^+ or ATP for 10 min. After addition of 1:500 protease inhibitor mixture (Sigma, cat. no. P8340) and 1:100 phosphatase inhibitor mixture (Sigma, cat. no. P2850), control and stimulated cells were lysed by sonication in ice for 1 min at 3 watts (Heat-System Ultrasonics, W380, New York). ADP-ribosyl cyclase activity was measured at 37 °C on cell lysates by adding 0.4 mM β-NAD^+. Aliquots (100 μl) were withdrawn at various times (0, 10, and 30 min), the reactions were stopped by addition of 220 μl of 0.9 M PCA to each aliquot, and the cADPR concentrations were measured by the enzymatic cycling assay (20). The protein content in each sample was determined by a Bradford assay (21).

siRNA Transfection—Transfection of human granulocytes was performed using the Nucleofector System (Amaxa GmbH, Cologne, Germany). Preliminary experiments were carried out with pmaxGFP to select the cell concentration, the Nucleofector solution, and program yielding the highest percentage of cell transfection, which was monitored by measuring GFP-positive cells. Moreover, viability of freshly isolated granulocytes was estimated at 24, 48, and 72 h measuring propidium iodide-positive cells by flow cytometry: the corresponding figures of cells viability were ~78%, 49 and 10%, respectively. Thus, the following protocols were chosen as optimal. Freshly isolated granulocytes (20×10^6 cells) were transfected without (control), or with 2 μM duplex short interference RNA (siRNA) or with 2 μg of pmaxGFP, using the Cell Line Nucleofector Kit T according to the manufacturer's instructions (Nucleofector program X-005). The control siRNA was obtained from Ambion (Austin, TX, negative control #1 siRNA). The $P2Y_{11}$-targeting siRNA was obtained from Invitrogen (P2RY11-HSS143212: 5′-UAUGUCUGCAAAGCUCGGGCAGCGG-3′). Immediately after transfection, cells were resuspended in 2.5 ml of RPMI supplemented with fetal calf serum (10%), penicillin (50 units/ml), and streptomycin (50 μg/ml) and incubated in a humidified 5% CO_2 atmosphere at 37 °C for 24 h. After 24 h, GFP-positive cells were evaluated by using FACSCanto flow cytometer (BD Biosciences), and data, expressed as percentage of alive, propidium iodide-negative cells, were analyzed by using DIVA software.

Real-time PCR—Twenty-four hours after transfection, total RNA was extracted from cells (2×10^6 cells) using the RNeasy mini kit (Qiagen) according to the manufacturer's instructions and reverse transcribed into cDNA using the Superscript III first strand synthesis system (Invitrogen). The cDNA was used as template for real-time PCR analysis: reactions were performed in an iCycler iQ5 real-time PCR detection system (Bio-Rad). The human $P2Y_{11}$-specific primers were designed by using Beacon Designer 2.0 software (Bio-Rad), and their sequences were as follows: 5′-CGTGAGCTGAGCCAATGATGTG-3′ (forward) and 5′-GGGTGGGAAAGGCGACTGC-3′ (reverse). Each sample was assayed in triplicate in a 25-μl amplification reaction, containing 30 ng of cDNA, primers mixture (0.4 μM each of sense and antisense primers), and 12.5 μl of 2× iQ SYBR Green Supermix Sample (Bio-Rad). The amplification program included 40 cycles of two steps, each comprising heating to 95 °C and to 60 °C, respectively. Fluorescent products were detected at the last step of each cycle. To verify the purity of the products, a melting curve was produced after each run. Values were normalized to β-actin mRNA expression. Statistical analysis of the quantitative real-time PCR was obtained using the iQ5 Optical System Software version 1.0 (Bio-Rad) based on the $2^{-\Delta\Delta Ct}$ method, which calculated relative changes in gene expression of the target ($P2Y_{11}$) normalized to β-actin and relative to a calibrator ("control," cells subjected to electroporation in the absence of siRNA). Amplification efficiencies of target and reference genes were determined by generating standard curves. Data are presented as means ± S.D.

Chemotaxis—Twenty-four hours after transfection, a 300-μl aliquot of granulocytes from each condition was centrifuged at 5000 × *g* for 10 s, and cells were resuspended at 7×10^6/ml in chemotaxis buffer (HBSS, phosphate-buffered saline, and 5% albumin, 39:16:1). Chemotaxis assays were performed using 96-well ChemoTx system microplates (Neuro Probe, Inc., Gaithersburg, MD) with a 3-μm pore size polycarbonate filter. α- or β-NAD^+ (10 μM) were diluted in chemotaxis buffer and added in the bottom wells. Granulocytes (25 μl) were placed on top of the filter and incubated for 60 min at 37 °C: the transmigrated cells were evaluated as previously described (12). The results were expressed as chemotaxis index (CI): CI = number of cells migrated toward chemoattractant/number of cells migrated toward medium.

Statistical Analyses—All parameters were tested by paired *t* test. *p* values <0.05 were considered significant.

RESULTS

Millimolar NAD^+_e Induces Both Transient and Sustained Ca^{2+} Responses in Human Granulocytes—Incubation of intact, freshly isolated granulocytes with extracellular β-NAD^+ (β-NAD^+_e) concentrations ranging from 1 to 100 μM resulted in a slowly developing, sustained elevation of $[Ca^{2+}]_i$ (12). As shown in Fig. 1 (*A* and *B*), a markedly different Ca^{2+} response was consistently observed upon incubating granulocytes with 1 mM β-NAD^+_e. Under these conditions, an immediate and transient elevation of the $[Ca^{2+}]_i$ (from 40 ± 6 to 105 ± 9 nM, $n = 5$) was followed by a sustained increase (to 145 ± 28 after 15 min from the addition of the nucleotide, $n = 5$).

When 1 mM β-NAD^+_e was added to granulocytes in the presence of 0.3 mM extracellular EGTA in Ca^{2+}-free HBSS, the kinetics and the extent of the immediate $[Ca^{2+}]_i$ increase were superimposable to those recorded in a Ca^{2+}-containing

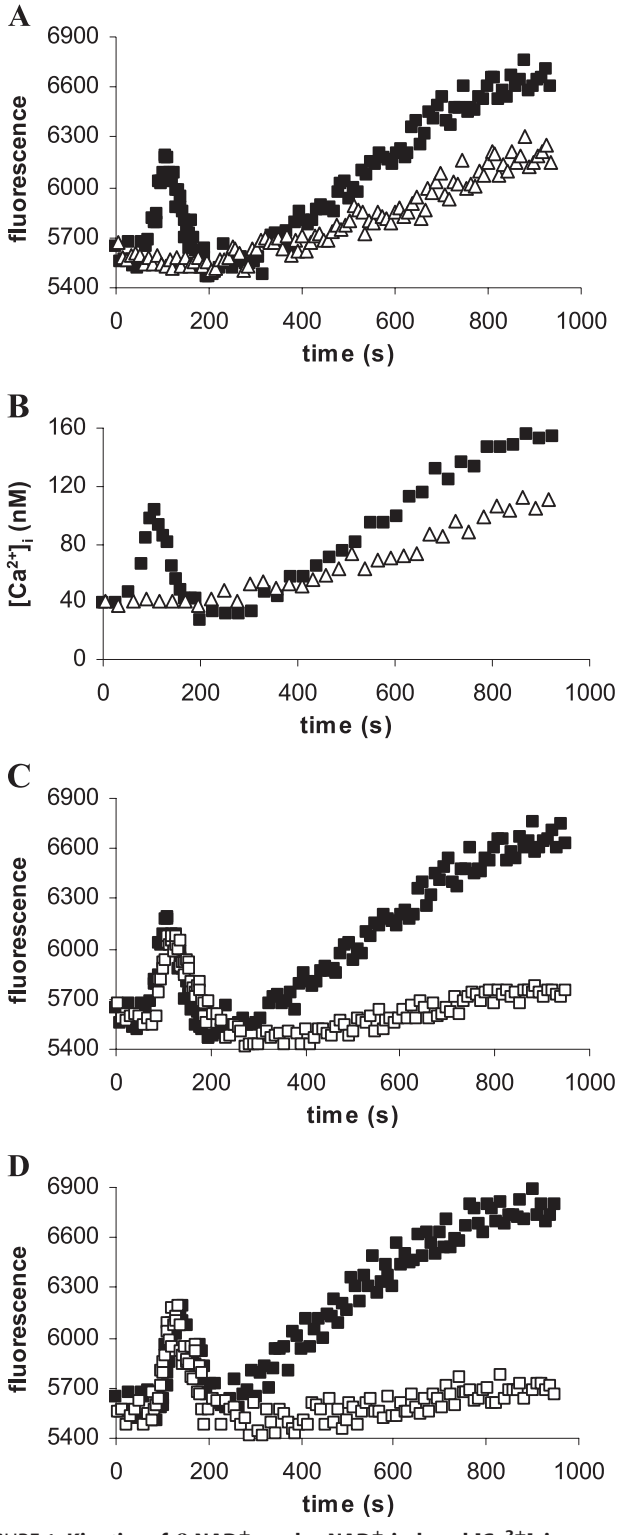

FIGURE 1. **Kinetics of β-NAD_e^+- and α-NAD_e^+-induced $[Ca^{2+}]_i$ increase in human granulocytes.** Fluo-3AM-loaded (*A*) or FURA-2AM-loaded (*B*) granulocytes were treated at 25 °C with 100 μM (*open triangles*) or 1 mM β-NAD^+ (*black squares*). Fluo-3AM-loaded granulocytes were treated at 25 °C with: *C*, 1 mM β-NAD^+ in calcium buffer (HBSS, *black squares*) or in HBSS containing 0.3 mM EGTA (*open squares*); *D*, 1 mM α-NAD^+ in calcium buffer (HBSS, *black squares*) or in HBSS containing 0.3 mM EGTA (*open squares*). $[Ca^{2+}]_i$ changes were measured in parallel using a fluorescence plate reader (*A*, *C*, and *D*), or with the system described in Ref. 12 for $[Ca^{2+}]_i$ calibration (*B*). Nucleotide was added at 50 s in *A* and *B* and at 70 s in *C* and *D*. Representative traces are shown (*A* and *C*, $n = 11$; *B*, $n = 5$; *D*, $n = 7$); *B*, each point is the mean of three $[Ca^{2+}]_i$ values, recorded every 9 s (S.D. $\leq$ 15% of the mean value).

medium (Fig. 1*C*), indicating that the transient increase in Ca^{2+} levels arises from release from intracellular stores and not from extracellular influx. By contrast, the sustained Ca^{2+} elevation triggered by millimolar β-NAD_e^+ was markedly decreased (80%) in the presence of EGTA, demonstrating that influx of extracellular Ca^{2+} is responsible for the sustained Ca^{2+} elevation at longer times (Fig. 1*C*), similar to what was observed with micromolar β-NAD_e^+ concentrations (12).

1 mM α-NAD_e^+ elicited the same two-step pattern of Ca^{2+} response as β-NAD_e^+ (Fig. 1*D*). Moreover, no appreciable quantitative differences were observed in the Ca^{2+} responses elicited by α-NAD_e^+ or β-NAD_e^+.

Distinct Roles of IP_3 and cADPR in Transient and Sustained Ca^{2+} Responses of Intact Granulocytes to NAD_e^+—Preincubation of intact granulocytes with the membrane-permeant phospholipase C (PLC) inhibitor (U73122, 5 μM) abolished the early transient $[Ca^{2+}]_i$ elevation promoted by either β-NAD_e^+ (Fig. 2*A*), or α-NAD_e^+ (not shown), whereas the same concentration of the inactive analog U73343 proved to be ineffective (Fig. 2*A*). Conversely, the sustained increase in $[Ca^{2+}]_i$ observed with α- and β-NAD_e^+ was not affected by pretreatment of the granulocytes with either U73122 or U73343. These findings demonstrate that α- and β-NAD_e^+ at 1 mM evoke a rapid Ca^{2+} release from IP_3-responsive intracellular stores.

To confirm the role of cADPR in the long lasting Ca^{2+} response induced by millimolar β-NAD_e^+, as was previously demonstrated with micromolar β-NAD_e^+ concentrations (12), intact granulocytes were exposed to β-NAD_e^+ (1 mM) following preincubation with either 8-Br-cADPR (100 μM), a membrane-permeant cADPR antagonist (22), or ryanodine at 50 μM, a concentration that inhibits Ca^{2+} release from cADPR-responsive stores (23). Although neither treatment affected the first, transient $[Ca^{2+}]_i$ increase, both 8-Br-cADPR and ryanodine significantly reduced (approximately by 80%) the sustained $[Ca^{2+}]_i$ elevation (Fig. 2, *B* and *C*). These results demonstrate that the sustained Ca^{2+} increase triggered by 1 mM NAD_e^+ is mediated by cADPR, similarly to what was observed at micromolar dinucleotide concentrations. This cADPR-dependent Ca^{2+} increase is abrogated in the presence of extracellular EGTA (Fig. 1).

Intracellular IP_3, cADPR, and cAMP Concentrations in NAD_e^+-stimulated Granulocytes—Exposure of granulocytes to 1 mM β-NAD_e^+ promoted a rapid increase in IP_3 levels. Following a 60-s incubation with the dinucleotide, intracellular IP_3 levels increased by ~2-fold, from a basal (unstimulated) value of 0.25 ± 0.03 pmol/10^6 to 0.54 ± 0.08 pmol/10^6 cells ($n = 3$, $p < 0.005$, Fig. 3*A*). Micromolar (10–100) concentrations of β-NAD_e^+ did not promote significant changes in IP_3 levels (data not shown). These data demonstrate the causal involvement of IP_3 generation in the initial, transient $[Ca^{2+}]_i$ increase in response to millimolar β-NAD_e^+ (Fig. 2*A*).

To investigate changes in cADPR levels promoted by millimolar NAD_e^+, we used α-NAD_e^+ as an agonist (12), which proved to be as effective as β-NAD_e^+ in triggering a pathway leading to stimulation of intracellular cADPR synthesis from β-NAD_i+ (12). α-NAD_e^+ was used to avoid possible interference of the measurement of intracellular cADPR levels by extracellular cADPR generated from β-NAD_e^+ (12). After a

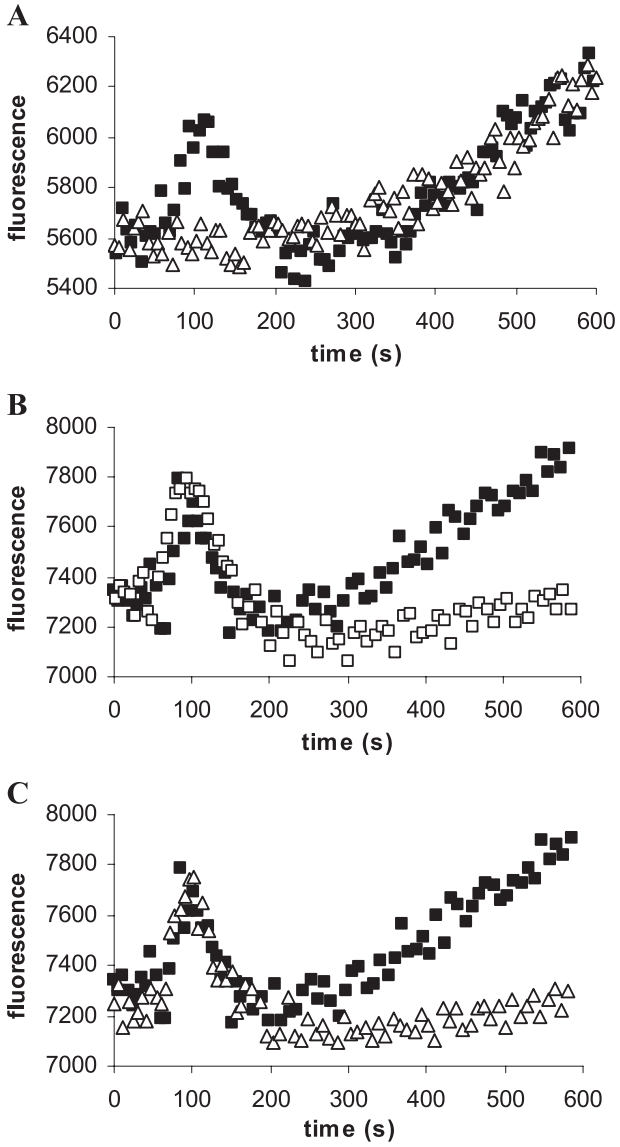

FIGURE 2. **Role of IP_3 and cADPR in the β-NAD_e^+-induced $[Ca^{2+}]_i$ increase in human granulocytes.** *A*, Fluo-3AM-loaded granulocytes were preincubated at 25 °C for 10 min in HBSS in the presence of 5 μM U73122 (*open triangles*) or U73343 (*black squares*). *B* and *C*, granulocytes were preincubated for 50 min in HBSS (control, *black squares*), or in HBSS containing 100 μM 8-Br-cADPR (*open squares*, *B*) or 50 μM ryanodine (*open triangles*, *C*) and then loaded for further 40 min with Fluo-3-AM. β-NAD^+ (1 mM) was then added, and $[Ca^{2+}]_i$ was measured in parallel using a fluorescence plate reader, as described under "Experimental Procedures." Nucleotide was added at 40 s in *A–C*. Representative traces are shown ($n \geq 3$ for each condition).

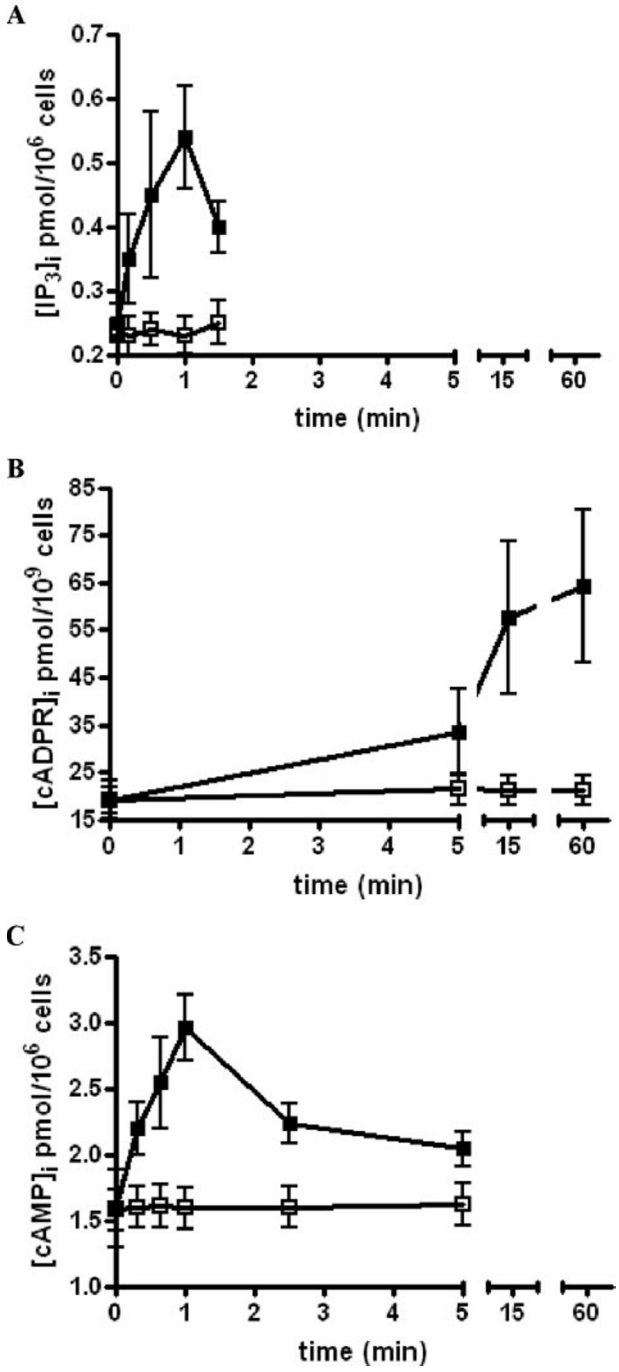

FIGURE 3. **Intracellular IP_3, cADPR, and cAMP levels in NAD_e^+-stimulated human granulocytes.** After addition of 1 mM β-NAD^+ to control, untreated granulocytes (*black squares*), or to cells preincubated for 1 h with 100 μM suramin (*open squares*), IP_3 (*A*), cADPR (*B*), and cAMP (*C*) levels were determined at the times indicated, as described under "Experimental Procedures." Results are the mean ± S.D. of at least three different experiments for each assay.

15-min exposure of granulocytes to 1 mM α-NAD_e^+, cADPR levels increased to 300 ± 80% ($n = 12$, $p < 0.001$) over basal levels (19.11 ± 4.01 pmol/10^9 cells, Fig. 3*B*), in agreement with the concentration-dependent effects observed at micromolar NAD_e^+ (12).

Stimulation of granulocyte ADPRC and the subsequent increase of $[cADPR]_i$ promoted by micromolar NAD_e^+ were shown to be dependent on the increase of cAMP and resulting PKA activation (12). Likewise, basal cAMP levels of human granulocytes (1.63 ± 0.35 pmol/10^6 cells, $n = 10$) increased immediately after cell stimulation with 1 mM β-NAD_e^+, reaching maximal values after 60 s (186 ± 16% of basal values, Fig. 3*C*). A comparable increase of the $[cAMP]_i$ was observed in α-NAD_e^+-stimulated cells (data not shown). Therefore, incubation of human granulocytes with millimolar NAD_e^+ resulted in comparably similar time course in elevation of intracellular IP_3 and cAMP levels (peaking at 60 s), whereas a longer time (15 min) was required for intracellular cADPR to reach a plateau.

Role of Purinergic Receptors in the NAD_e^+-induced Ca^{2+} Responses of Intact Granulocytes—Recently, a role for purinergic receptors in nucleotide-triggered Ca^{2+} responses or Ca^{2+}-

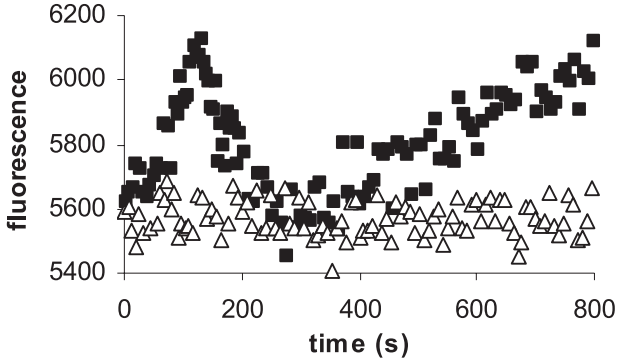

FIGURE 4. **Effect of suramin on the β-NAD$_e^+$-induced [Ca^{2+}]$_i$ increase in human granulocytes.** Control, untreated (*black squares*) or suramin-treated (100 μM for 1 h, *open triangles*) granulocytes were loaded with Fluo-3AM and exposed to 1 mM β-NAD$^+$ at 25 °C. [Ca^{2+}]$_i$ changes were measured in parallel using a fluorescence plate reader, as described under "Experimental Procedures." Nucleotide was added at 40 s. Representative traces are shown ($n = 5$).

regulated cell functions in blood cells (24), dendritic cells (25), and T lymphocytes (7, 10, 11) has emerged. To address the type of receptors that mediate the NAD$_e^+$-induced Ca^{2+} responses in human granulocytes, intact cells were preincubated with suramin, a widely used antagonist of both G protein-coupled P2Y and ion channel-forming P2X receptors (24, 26). To investigate the specificity of suramin as a P2Y receptor inhibitor in our cell system, granulocytes were first incubated in the presence of suramin (100 μM for 1 h) and then incubated with either 100 μM ATP, 1 μM fMLP, or 1 μM A5 peptide (15). Indeed, suramin strongly inhibited (87%, $n = 3$) the ATP-induced Ca^{2+} increase, whereas little to no changes in the P2Y-unrelated Ca^{2+} responses to fMLP and A5 peptide were observed (15 and 0% inhibition, respectively, $n = 3$, data not shown).

Preincubation of human granulocytes with suramin resulted in complete abrogation of the rapid, transient NAD$_e^+$-promoted increase in intracellular Ca^{2+} (Fig. 4). This finding, together with the complete inhibition afforded by the PLC inhibitor U73122 (Fig. 2*A*), suggested that the transient increase of [Ca^{2+}]$_i$ promoted by millimolar NAD$_e^+$ was due to engagement of a PLC-coupled P2Y receptor. Consistent with this hypothesis, suramin strongly inhibited NAD$_e^+$-promoted increases in IP$_3$ levels (Fig. 3*A*).

Interestingly, the slow, sustained elevation of [Ca^{2+}]$_i$ elicited by 1 mM β-NAD$_e^+$ was also strongly inhibited (80 ± 5%) by suramin (Fig. 4). Thus, we explored the effect of suramin on cAMP levels in granulocytes stimulated with 1 mM β-NAD$_e^+$. Indeed, preincubation with suramin resulted in complete inhibition of cAMP generation (Fig. 3*C*). Likewise, preincubation of granulocytes with suramin resulted in almost complete inhibition of NAD$_e^+$-promoted increases in cADPR (Fig. 3*B*), suggesting that a suramin-inhibitable receptor, triggered by 1 mM NAD$_e^+$, lies upstream of the activation of AC and of ADPRC. Taken together, these data demonstrate that in human granulocytes a suramin-inhibitable purinoceptor mediates both the rapid, transient, and IP$_3$-dependent elevation of [Ca^{2+}]$_i$ and the subsequent slow, sustained cAMP/PKA/cADPR-dependent elevation of [Ca^{2+}]$_i$ promoted by millimolar NAD$_e^+$.

Extracellular NAD⁺ Increases the [Ca^{2+}]$_i$ of P2Y$_{11}$-1321N1 Astrocytoma Cells—Among the human G protein-coupled P2Y receptor (hP2Y) subtypes cloned to date, only the hP2Y$_{11}$ receptor couples to both PLC and adenylyl cyclase (16). To establish whether the P2Y$_{11}$ receptor is activated by NAD$_e^+$, we investigated the effect of the dinucleotide on [Ca^{2+}]$_i$ in 1321N1 human astrocytoma cells stably expressing the hP2Y$_{11}$ receptor (1321N1-hP2Y$_{11}$ cells) (17). To rule out possible interferences afforded by metabolic by-products of NAD$_e^+$ (*e.g.* ADPR, AMP, and adenosine), we investigated the stability of α- and β-NAD$_e^+$ during incubation with both native 1321N1 and 1321N1-hP2Y$_{11}$ cells. Importantly, no significant degradation of either dinucleotide form (100 μM) was observed over 60 min at 25 °C.

Addition of 100 μM β-NAD$_e^+$ to 1321N1-hP2Y$_{11}$ cells promoted a rapid and transient increase of [Ca^{2+}]$_i$, followed by a slow, sustained [Ca^{2+}]$_i$ rise. Conversely, β-NAD$_e^+$ did not induce any Ca^{2+} response on control 1321N1 cells (Fig. 5*A*), indicating that the P2Y$_{11}$ receptor was responsible for the NAD$_e^+$-promoted transient and sustained increases of [Ca^{2+}]. In agreement with results obtained with human granulocytes, the rapid and transient NAD$_e^+$-promoted elevation in [Ca^{2+}]$_i$ was due to release from intracellular stores, because it was not abrogated in the presence of extracellular EGTA. In contrast, the sustained [Ca^{2+}]$_i$ rise elicited by NAD$_e^+$ was completely inhibited by extracellular EGTA, implicating Ca^{2+} influx (data not shown). Ca^{2+} mobilization was also observed in 1321N1-hP2Y$_{11}$ cells challenged with extracellular ATP. The kinetics of the Ca^{2+} response was similar to those observed with NAD$_e^+$, although consistently more robust (Fig. 5*A*).

Preincubation of 1321N1-hP2Y$_{11}$ cells with either the PLC inhibitor, U73122, or with suramin completely abrogated the rapid and transient increase in [Ca^{2+}]$_i$ (Fig. 5, *B* and *C*), confirming the involvement of the PLC-coupled P2Y$_{11}$ receptor in triggering the rapid [Ca^{2+}]$_i$ rise. Suramin also abrogated the slow and sustained [Ca^{2+}]$_i$ elevation, whereas the PLC inhibitor was ineffective (Fig. 5, *B* and *C*). These results indicate that the sustained [Ca^{2+}]$_i$ rise is also triggered by the P2Y$_{11}$ receptor, yet via a PLC-independent pathway. The sustained Ca^{2+} increase, which was due to extracellular Ca^{2+} influx, was inhibited by preincubation of 1321N1-hP2Y$_{11}$ cells with 8-Br-cADPR (Fig. 5*D*), in agreement with previous data obtained for human granulocytes (12).

Challenging 1321N1-hP2Y$_{11}$ cells with ATP (100 μM) instead of NAD$^+$ had no effect on the action of the various inhibitors on the biphasic Ca^{2+} response. Thus, suramin inhibited almost completely (80 ± 5%, $n = 3$) both the rapid and sustained increases in [Ca^{2+}]$_i$, whereas U73122 abrogated only the rapid, transient phase ($n = 3$) and 8-Br-cADPR strongly reduced (73 ± 8%, $n = 3$) only the slowly developing sustained phase of ATP-promoted [Ca^{2+}]$_i$ increase (data not shown). The sustained [Ca^{2+}]$_i$ increases induced by both β-NAD$_e^+$ (100 μM) and ATP (100 μM) in 1321N1-hP2Y$_{11}$ cells were completely inhibited by SKF96365 (10 μM, 1-min preincubation), an inhibitor of store-operated calcium channels (27).

Extracellular NAD⁺ Increases Intracellular IP$_3$, cAMP, and cADPR Levels in 1321N1-hP2Y$_{11}$ Cells—The results described above clearly indicate the activation by β-NAD$_e^+$ of an IP$_3$- and a cAMP/cADPR-dependent pathway leading to discrete Ca^{2+} responses in hP2Y$_{11}$-1321N1 cells. The hP2Y11 receptor expressed by 1321N1 cells is indeed known to be coupled to both PLC and AC (16).

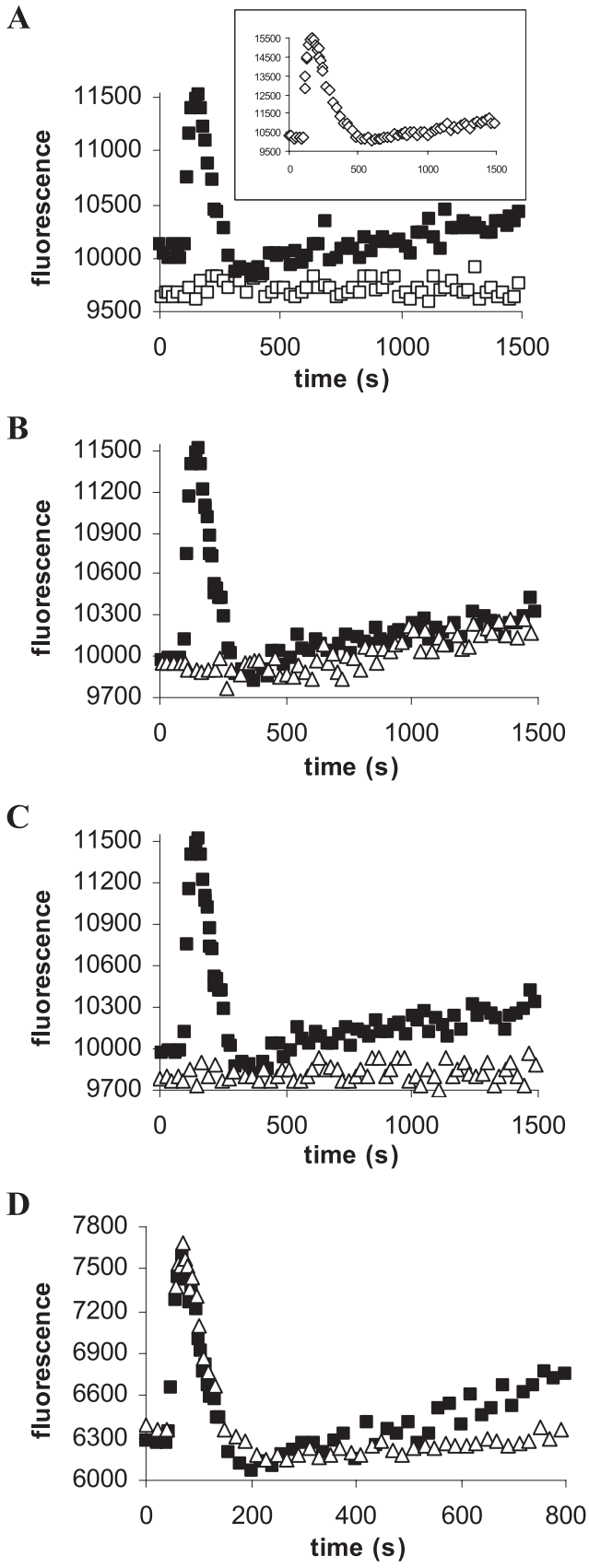

FIGURE 5. **β-NAD_e^+- and ATP-induced $[Ca^{2+}]_i$ increase in $hP2Y_{11}$-1321N1 cells.** *A*, Fluo-3AM-loaded $hP2Y_{11}$-1321N1 cells were treated with 100 μM β-NAD_e^+ (*black squares*) or with 100 μM ATP_e (*open rhombus*, *inset*); control 1321N1 cells were exposed to 100 μM β-NAD_e^+ (*open squares*); *B*, untreated (*black squares*) or U73122 preincubated (5 μM for 10 min, *open triangles*) $hP2Y_{11}$-1321N1 cells were incubated with 100 μM β-NAD_e^+; *C*, untreated (*black squares*) or suramin preincubated (100 μM for 1 h, *open triangles*) $hP2Y_{11}$-1321N1 cells were challenged with 100 μM β-NAD_e^+; *D*, untreated (*black squares*) or 8-Br-cADPR preincubated (100 μM for 90 min, *open triangles*) $hP2Y_{11}$-1321N1 cells were incubated with 100 μM β-NAD_e^+. $[Ca^{2+}]_i$ changes were measured in parallel at 25 °C using a fluorescence plate reader, as described under "Experimental Procedures." Nucleotide was added at 70 s in *A–C* and at 40 s in *D*. Representative traces are shown (*A*, $n = 8$; *B–D*, $n = 5$).

TABLE 1

β-NAD_e^+-induced intracellular IP_3, cAMP, and cADPR increases in $hP2Y_{11}$-1321N1 cells

β-NAD^+ was added at the concentrations indicated to $hP2Y_{11}$-1321N1 cells, IP_3 levels were determined after 30 s from the addition of β -NAD_e^+ ($n = 4$), cAMP levels were determined after 15 min from the addition of β -NAD_e^+ ($n = 6$), and cADPR levels were measured in lysates from cells incubated for 15 min with α-NAD^+ ($n = 5$), as described under "Experimental Procedures." Results are the mean ± S.D.

$\beta-NAD_e^+$	IP_3	cAMP	cADPR
μM		*pmol/10⁶ cells*	
0	23.58 ± 3.67	2.53 ± 0.45	0.227 ± 0.054
10	31.54 ± 3.08[a]	3.70 ± 0.41[a]	0.262 ± 0.035
100	38.43 ± 3.30[b]	10.11 ± 1.06[b]	0.329 ± 0.049[a]

[a] $p < 0.05$.
[b] $p < 0.001$.

To conclusively demonstrate the role of IP_3, cAMP, and cADPR in the $[Ca^{2+}]_i$ responses triggered by NAD_e^+-induced activation of $P2Y_{11}$, we measured the intracellular concentrations of these second messengers following NAD_e^+ stimulation of $hP2Y_{11}$-1321N1 cells.

Challenge of 1321N1-$hP2Y_{11}$ cells with 10 and 100 μM β-NAD_e^+ caused a steady elevation of IP_3 levels, reaching 134 and 163% of basal values, respectively, recorded in unstimulated cells (Table 1) and measured 30 s after addition of agonist. By contrast, the same concentration of ATP induced a 3-fold increase in IP_3 levels in 1321N1-$hP2Y_{11}$ cells. In native 1321N1 cells, the basal value of $[IP_3]_i$ (8.79 ± 1.32 pmol/10^6 cells) was not significantly modified by incubation with 100 μM β-NAD_e^+.

Because the $hP2Y_{11}$ receptor is coupled to both G_q and G_s (16), we determined whether NAD^+ increased cAMP levels in native 1321N1 and 1321N1-$hP2Y_{11}$ cells. Following a 15-min incubation with 100 μM β-NAD_e^+, cAMP levels increased from a basal value of 2.53 ± 0.45 pmol/10^6 cells to 10.11 ± 1.06 pmol/10^6 cells (Table 1). Concentrations as low as 10 μM β-NAD_e^+ were capable of stimulating a significant increase in cAMP (Table 1). In contrast to the effects induced by β-NAD^+, stimulation of 1321N1-$hP2Y_{11}$ cells with 100 μM ATP for 15 min resulted in a much greater increase in cAMP (to 196 ± 41 pmol/10^6 cells, $n = 5$). cAMP levels measured in control 1321N1 cells were not significantly increased in the presence of 100 μM NAD^+.

We next investigated whether elevations in cAMP in NAD^+-stimulated 1321N1-$hP2Y_{11}$ cells are responsible for the slowly developing, sustained $[Ca^{2+}]_i$ rise through the NAD_e^+-triggered signaling pathway described in human granulocytes (12). For this purpose, Fluo-3AM-loaded 1321N1-$hP2Y_{11}$ cells were incubated in the presence of the cell-permeant PKA activator, 8-Br-cAMP (500 μM). As shown in Fig. 6, a sustained $[Ca^{2+}]_i$ increase was recorded within 4 min of 8-Br-cAMP addition ($n = 3$), similar to that previously described in human granulo-

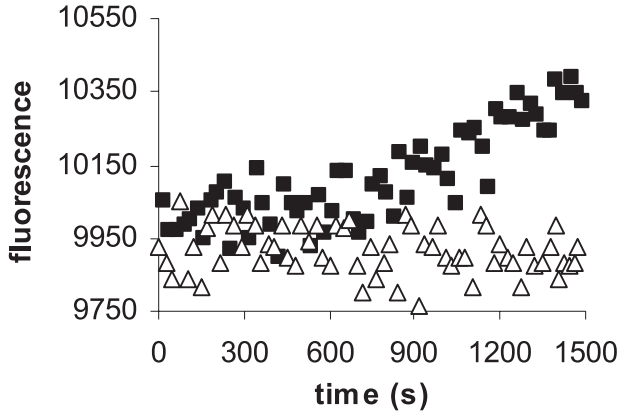

FIGURE 6. **8-Br-cAMP-induced $[Ca^{2+}]_i$ increase in hP2Y$_{11}$-1321N1 cells.** Traces shown, representative of three different experiments, were obtained upon addition (at 300 s) of 500 μM 8-Br-cAMP (*black squares*) to Fluo-3AM-loaded hP2Y$_{11}$-1321N1 cells. *Open triangles* indicate the same cells without addition of 8-Br-cAMP. $[Ca^{2+}]_i$ changes were measured in parallel at 25 °C using a fluorescence plate reader.

cytes (12). A comparable sustained $[Ca^{2+}]_i$ increase was also obtained upon addition of 500 μM 8-Br-cAMP to control 1321N1 cells (not shown).

The inhibition of the sustained increase in $[Ca^{2+}]_i$ afforded by 8-Br-cADPR (Fig. 5*D*) prompted us to measure the effects of NAD^+ on both ADPRC activity (responsible for cADPR generation from β-NAD^+) and on levels of cADPR in 1321N1-hP2Y$_{11}$ cells. Cells were incubated for 10 min in the presence or absence of 100 μM α-NAD_e^+ (which is not a substrate of any known ADPRC (28)), and levels of ADPRC activity were then measured in cell lysates using β-NAD^+ as substrate. ADPRC activity increased from 0.10 ± 0.03 in unstimulated 1321N1-hP2Y$_{11}$ cells to 0.23 ± 0.05 pmol of cADPR/min/mg of protein in α-NAD^+-treated cells ($n = 3$, $p < 0.01$). Conversely, no increase of the ADPRC activity was recorded in P2Y11$^-$ cells stimulated with α-NAD_e^+ (not shown).

Likewise, following a 15-min addition of 100 μM α-NAD_e^+ to 1321N1-hP2Y$_{11}$ cells, the levels of cADPR increased to 145 ± 22% of basal value (0.23 ± 0.05 pmol/10^6 cells) (Table 1). Similar results were obtained when 1321N1-hP2Y$_{11}$ cells were exposed for 15 min to 100 μM ATP (increase to 0.33 ± 0.08 pmol/10^6 cells, $n = 4$). Conversely, cADPR levels in control 1321N1 cells (basal value, 0.22 ± 0.05 pmol/10^6 cells, $n = 3$) were not significantly increased by 100 μM α-NAD_e^+.

Role of Endogenous P2Y$_{11}$ in NAD⁺-induced Activation of Human Granulocytes—To demonstrate that endogenous P2Y$_{11}$ is the receptor responsible for the NAD^+-induced Ca^{2+} response leading to activation of human granulocytes, we followed two different experimental approaches. First, cells were preincubated with 1 μM NF157, a selective and potent P2Y$_{11}$ receptor antagonist: as reported by Ullmann *et al.* (19), 1 μM NF157 does not affect the P2Y$_2$ purinoceptor, *i.e.* the receptor involved in the ATP-induced activation of human granulocytes (29). Second, down-regulation of P2Y$_{11}$ expression in human granulocytes was achieved by means of specific siRNA transfection.

Preincubation of human granulocytes with NF157 resulted in the abrogation of the sustained $[Ca^{2+}]_i$ increase induced by 100 μM β-NAD^+ (not shown). Moreover, the presence of NF157 completely prevented the transient $[Ca^{2+}]_i$ elevation triggered by 1 mM β-NAD^+ and strongly inhibited (81 ± 5%) the sustained $[Ca^{2+}]_i$ increase induced by 1 mM β-NAD^+ (Fig. 7*A*). At the same time, the presence of NF157 abrogated the NAD_e^+-promoted increases in IP_3 and cAMP levels (Fig. 7, *B* and *C*). Similar results were obtained upon stimulation of granulocytes with α-NAD^+ (not shown). In addition, as shown in Fig. 7*D*, preincubation of cells with NF157 strongly inhibited chemotaxis of human granulocytes toward 10 μM α- or β-NAD^+, the concentration triggering the maximal chemotactic response (12).

Next, human granulocytes were transfected with specific siRNA for P2Y$_{11}$: after 24 h, P2Y$_{11}$ mRNA levels were decreased to ~20% compared with control cells (electroporated in the absence of siRNA), as confirmed by real-time PCR analysis (Fig. 8*A*). The presence of a negative control siRNA did not induce any significant modification of P2Y$_{11}$ mRNA levels in human granulocytes (Fig. 8*A*). The NAD_e^+-induced Ca^{2+} responses were then measured at 24 h after transfection: as shown in Fig. 8*B*, down-regulation of P2Y$_{11}$ was accompanied by the almost complete inhibition of both Ca^{2+} responses triggered by 1 mM β-NAD^+, *i.e.* the IP_3-related rapid increase and the cADPR-dependent sustained rise. Comparable results were obtained upon stimulation of cells with 1 mM α-NAD^+ (not shown). Finally, P2Y$_{11}$ siRNA-transfected, negative control siRNA-transfected, and control granulocytes were comparatively challenged to migrate toward 10 μM α- or β-NAD^+: as shown in Fig. 8*C*, transfection with specific siRNA for P2Y$_{11}$ completely prevented chemotaxis of granulocytes.

DISCUSSION

The recent discovery of NAD^+ as an extracellular agonist eliciting functional activation of human granulocytes (12) highlighted a new mechanism for this dinucleotide, which was distinct from its action in other mammalian cell types (1–8). In astrocytes, osteoblasts, CD38-transfected fibroblasts, and HeLa cells, CD38, an ecto-ADPRC, converts NAD_e^+ into the intracellular calcium mobilizer cADPR (1, 3, 5, 6). Subsequent translocation of extracellularly generated cADPR into the cytoplasm, where it can cause release of Ca^{2+} stores by binding to the ryanodine receptor, is performed either by CD38 itself or by nucleoside transporters (1). In murine T lymphocytes, the addition of NAD_e^+ promotes Ca^{2+} influx secondary to NAD_e^+-mediated ADP ribosylation of the P2X$_7$ purinoceptor or of a P2X-associated protein (7, 10, 11).

In contrast, the $[Ca^{2+}]_i$ increase in human granulocytes promoted by micromolar NAD_e^+ occurs through (i) overproduction of cAMP, (ii) activation of PKA, (iii) stimulation of ADPRC activity and consequent overproduction of cADPR, and (iv) influx of extracellular Ca^{2+} (12). Functional equivalence between β-NAD_e^+ and α-NAD_e^+, which is not a substrate of either ADPRCs (28) or ADP-ribosyl transferases (30), suggested that NAD_e^+ activates one or more plasma membrane receptors coupled to a signaling pathway that result in granulocyte activation. However, identification of such receptor(s) has remained elusive (12).

The results obtained in this study demonstrate for the first time that NAD_e^+ is an endogenous agonist of the P2Y$_{11}$ purinoceptor and that engagement of P2Y$_{11}$ by extracellular NAD^+

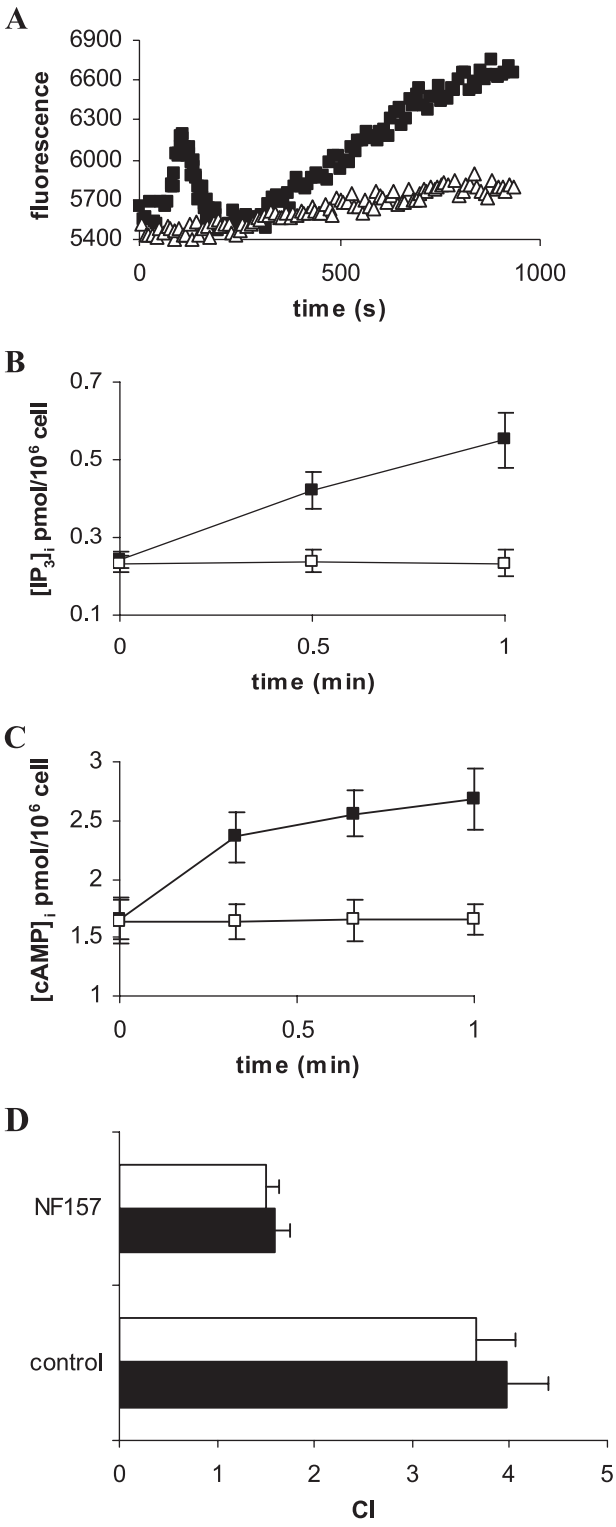

FIGURE 7. **Effect of NF157 on the NAD_e^+-induced $[Ca^{2+}]_i$, $[IP_3]_i$ and $[cAMP]_i$ increases and on NAD^+-directed chemotaxis in human granulocytes.** *A*, control, untreated (*black squares*) or NF157-treated (1 μM for 1 h, *open triangles*) granulocytes were loaded with Fluo-3AM and exposed to 1 mM β-NAD^+ at 25 °C. $[Ca^{2+}]_i$ changes were measured in parallel using a fluorescence plate reader, as described under "Experimental Procedures." Nucleotide was added at 70 s. Representative traces are shown ($n = 3$). After addition of 1 mM β-NAD^+ to control, untreated granulocytes (*black squares*), or to cells preincubated for 1 h with 1 μM NF157 (*open squares*), both IP_3 (*B*) and cAMP (*C*) levels were determined at the times indicated, as described under "Experimental Procedures." Results are the mean ± S.D. of at least three different experiments for each assay. *D*, migration of granulocytes preincubated, or not (control), with NF157 (1 μM for 40 min) through 3-μm pore membranes toward a medium containing, or not, 10 μM β-NAD^+ (*black bars*) or α-NAD^+ (*white bars*), was measured in ChemoTx chambers and the chemotaxis index (*CI*) was calculated. Migration of NF157-pretreated granulocytes toward the medium in the absence of NAD^+ was not significantly different from that of control, untreated cells. Results shown are the mean ± S.D. of four experiments ($p < 0.005$).

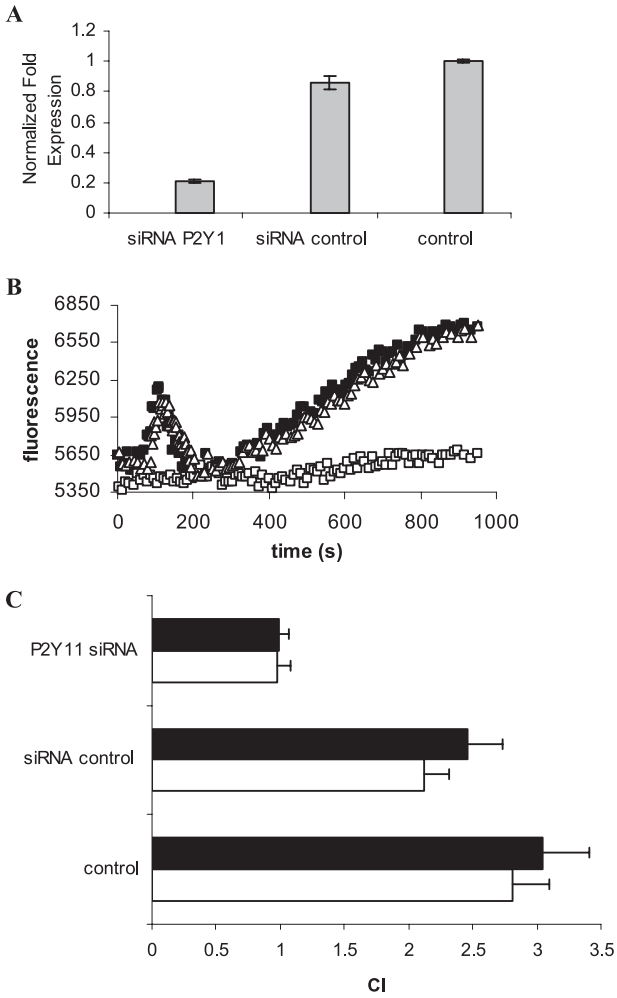

FIGURE 8. **Effect of siRNA for $P2Y_{11}$ on the NAD_e^+-induced $[Ca^{2+}]_i$ increases and NAD^+-directed chemotaxis in human granulocytes.** 24 h after transfection, control (electroporated in the absence of siRNA), negative control siRNA-transfected, or $P2Y_{11}$ siRNA-transfected granulocytes were treated as follows. *A*, subjected to total RNA extraction: real-time PCR for $P2Y_{11}$ expression was performed as described under "Experimental Procedures" ($n = 3$); *B*, loaded with Fluo-3AM and exposed to 1 mM β-NAD^+ at 25 °C (control, *black squares*; control siRNA, *open triangles*; $P2Y_{11}$ siRNA, *open squares*). $[Ca^{2+}]_i$ changes were measured in parallel using a fluorescence plate reader, as described under "Experimental Procedures." Nucleotide was added at 70 s. Representative traces are shown ($n = 3$); *C*, challenged to migrate toward a medium containing, or not, 10 μM β-NAD^+ (*black bars*) or α-NAD^+ (*white bars*). Migration was measured in ChemoTx chambers, and the chemotaxis index (*CI*) was calculated. Migration of transfected granulocytes toward the medium in the absence of NAD^+ was not significantly different from that of control cells. Results shown are the mean ± S.D. of three experiments ($p < 0.001$).

triggers a cADPR-dependent Ca^{2+} signaling eventually leading to activation of human granulocytes. Both conclusions are supported by several biochemical, pharmacological, and molecular lines of evidence. A first clue came from the finding of different patterns of $[Ca^{2+}]_i$ variations induced by micromolar and millimolar NAD_e^+ concentrations. The two steps of Ca^{2+} mobili-

zation proved to involve independent, not causally interrelated mechanisms, because the fast, IP_3-mediated increase in $[Ca^{2+}]_i$ was not necessary to induce the subsequent sustained $[Ca^{2+}]_i$ rise. These results indicated that the role of the cAMP/cADPR pathway is predominant at micromolar NAD^+_e over the PLC/IP_3 cascade. Activation of both signaling pathways by millimolar NAD^+_e concentrations suggested two alternative explanations: (*a*) binding of high $[NAD^+]_e$ to two different plasma membrane receptors, each of which couples to a distinct signaling cascade and (*b*) interaction of NAD^+_e with a single receptor coupling to both pathways of the Ca^{2+} response.

NAD^+ *per se* has never been demonstrated to be a ligand of purinoceptors, although it bears structural similarity with the classic agonists of purinoceptors, ADP and ATP. P2 (nucleotide) receptors encompass the ion channel forming P2X receptors and the G protein-coupled P2Y receptors. Whereas the seven subtypes of P2X receptors ($P2X_{1-7}$) are primarily activated by ATP, the eight subtypes of P2Y receptors ($P2Y_{1,2,4,6,11-14}$) are activated by a wider range of nucleotides and nucleotide analogs (26).

The abrogation of all the β-NAD^+-promoted effects by suramin, a non-selective inhibitor of the family of P2 receptors (24, 26), suggested the possibility that NAD^+_e was an agonist at one or more P2Y receptors; indeed, P2Y receptors are involved in PLC and/or AC activation (26). Human granulocytes express $P2Y_2$, $P2Y_4$, $P2Y_6$, and $P2Y_{11}$ receptor subtypes, as revealed by reverse transcription-PCR analysis (29). $P2Y_2$, $P2Y_4$, and $P2Y_6$ receptors are coupled to PLC, resulting in the formation of IP_3 and mobilization of $[Ca^{2+}]_i$, as well as activation of PKC (31). Notably, distinct from other members of the P2Y subfamily, the human $P2Y_{11}$ receptor is functionally coupled to both PLC and AC (16).

The unambiguous association of any P2Y receptor subtype with a specific physiological effect is hampered by the lack of subtype-selective agonists and antagonists (17). Thus, the pharmacological selectivities of these receptors can be optimally defined by expressing individual subtypes of cloned P2Y receptors in null cells. In our study, an astrocytoma cell line (1321N1) expressing the human $P2Y_{11}$ (17) was exploited to determine the possible activation of this receptor by NAD^+_e. Indeed, native 1321N1 astrocytoma cells lack expression of any known P2 receptor subtypes (32). β-NAD^+_e triggers both the cAMP/cADPR and the PLC/IP_3 pathways in 1321N1-h$P2Y_{11}$ cells but not in native 1321N1 cells.

The fact that the h$P2Y_{11}$ receptor is the only purinoceptor coupled to AC, together with its known expression in granulocytes, implicated the h$P2Y_{11}$ receptor as the putative receptor responsive to NAD^+_e in these cells. This view received experimental support by use of NF157, a suramin-related $P2Y_{11}$-selective antagonist, which was recently synthesized and characterized (19). Indeed, 1 μM NF157 abrogated in granulocytes both Ca^{2+} responses elicited by millimolar NAD^+_e (Fig. 7*A*).

Final evidence for the identification of $P2Y_{11}$ as the NAD^+-binding purinoceptor that mediates granulocyte activation was provided by specific siRNA transfection (Fig. 8). A significant decrease in $P2Y_{11}$ mRNA levels, observed 24 h after transfection with specific siRNA, indicates a relatively high turnover of $P2Y_{11}$ in human granulocytes (Fig. 8*A*). The experiments with $P2Y_{11}$-specific siRNA unequivocally identified $P2Y_{11}$ as the receptor interacting with NAD^+_e.

Previous studies performed on 1321N1-h$P2Y_{11}$ astrocytoma cells provided information on the pharmacological properties of this purinoceptor, demonstrating that it couples to AC and PLC with different efficiencies depending on the used agonist (16, 17). Specifically, previous data demonstrated that coupling of $P2Y_{11}$ with AC was triggered by ADP with a lower potency than by ATP as an agonist (17), whereas UTP stimulation did not lead to accumulation of IP_3, under conditions in which ATP gave a robust effect (33).

From the standpoint of agonist activity, it is of potential biological interest that, like β-NAD^+_e, micromolar ATP_e also evoked both an initial IP_3-dependent Ca^{2+} spike and a cADPR-dependent sustained $[Ca^{2+}]_i$ rise in 1321N1-h$P2Y_{11}$ cells. The ATP-promoted sustained rise in intracellular Ca^{2+} was significantly higher than that evoked by β-NAD^+_e (Fig. 5*A*); this difference might be accounted for by the greater depletion of intracellular Ca^{2+} stores elicited by ATP via IP_3 overproduction (34), as suggested by experiments with SKF96365 (see "Results"). cADPR was involved in the slowly developing sustained rise in $[Ca^{2+}]_i$ promoted by both β-NAD^+_e and ATP_e, as demonstrated by the substantial inhibition afforded by 8-Br-cADPR. Previous reports have postulated the occurrence of a cADPR-mediated activation of store-operated calcium channels (12, 14, 35–38). In recent years, growing evidence has accumulated that strongly implicates the TRPM2 channels as responsible for cADPR- and ADPR-mediated Ca^{2+} influx (39, 40).

The causal role of cADPR in the sustained $[Ca^{2+}]_i$ rise induced by both NAD^+_e and ATP_e in the h$P2Y_{11}$-132N1 cells is well established. However, it is somewhat surprising that the increase of intracellular cADPR in the h$P2Y_{11}{}^+$ cells was not much greater with ATP than with NAD^+_e (see "Results"). This seems to contrast with the different extents of $[cAMP]_i$ elevation in response to β-NAD^+_e and ATP_e, respectively, with ATP being far more potent and efficacious in stimulating cAMP overproduction. A possible explanation for this quantitative discrepancy might be the attainment of near-maximal activation of PKA at the $[cAMP]_i$ levels induced by β-NAD^+_e.

In conclusion, the present study demonstrates that β-NAD^+_e is an endogenous agonist of the $P2Y_{11}$ purinergic receptor, acting as a pro-inflammatory cytokine on human granulocytes. In this respect, increased levels of NAD^+_e and ATP expected at sites of inflammation, as a consequence of cell lysis (11) or of regulated release (41, 42), are likely to be sufficient to trigger functional responses in granulocytes, particularly enhanced chemotaxis, that are causally related to the cADPR/Ca^{2+} system (12). Specifically, as far as NAD^+_e concentrations are concerned, these average 50–100 nM in human blood plasma (1), thus close to those resulting in enhanced chemotaxis (12). *In vivo*, the extent of cell lysis as a source of NAD^+_e at specific sites can only be postulated, but hardly estimated. Conversely, the established capacity of increased $[Ca^{2+}]_i$ of down-regulating intracellular NAD^+ release via PKC-mediated phosphorylation of Cx43 hemichannels (43) might suggest the opposite process, *i.e.* opening of these hemichannels via dephosphorylation and consequently enhanced efflux of NAD^+ from cells.

REFERENCES

1. De Flora, A., Zocchi, E., Guida, L., Franco, L., and Bruzzone, S. (2004) *Ann. N. Y. Acad. Sci.* **1028,** 176–191
2. Ziegler, M., and Niere, M. (2004) *Biochem. J.* **382,** 5–6
3. Verderio, C., Bruzzone, S., Zocchi, E., Fedele, E., Schenk, U., De Flora, A., and Matteoli, M. (2001) *J. Neurochem.* **78,** 1–13
4. Esguerra, M., and Miller, R. F. (2002) *Glia* **39,** 314–319
5. Sun, L., Adebanjo, O. A., Moonga, B. S., Corisdeo, S., Anandatheerthavarada, H. K., Biswas, G., Arakawa, T., Hakeda, Y., Koval, A., Sodam, B., Bevis, P. J., Moser, A. J., Lai, F. A., Epstein, S., Troen, B. R., Kumegawa, M., and Zaidi, M. (1999) *J. Cell Biol.* **146,** 1161–1172
6. Romanello, M., Bicego, M., Pirulli, D., Crovella, S., Moro, L., and D'Andrea, P. (2002) *Biochem. Biophys. Res. Commun.* **299,** 424–431
7. Seman, M., Adriouch, S., Scheuplein, F., Krebs, C., Freese, D., Glowacki, G., Deterre, P., Haag, F., and Koch-Nolte, F. (2003) *Immunity* **19,** 571–582
8. Gerth, A., Nieber, K., Oppenheimer, N. J., and Hauschildt, S. (2004) *Biochem. J.* **382,** 849–856
9. Lee, H. C., Walseth, T. F., Bratt, G. T., Hayes, R. N., and Clapper, D. L. (1989) *J. Biol. Chem.* **264,** 1608–1615
10. Kawamura, H., Aswad, F., Minagawa, M., Malone, K., Kaslow, H., Koch-Nolte, F., Schott, W. H., Leiter, E. H., and Dennert, G. (2005) *J. Immunol.* **174,** 1971–1979
11. Krebs, C., Adriouch, S., Braasch, F., Koestner, W., Leiter, E. H., Seman, M., Lund, F. E., Oppenheimer, N., Haag, F., and Koch-Nolte, F. (2005) *J. Immunol.* **174,** 3298–3305
12. Bruzzone, S., Moreschi, I., Guida, L., Usai, C., Zocchi, E., and De Flora, A. (2006) *Biochem. J.* **393,** 697–704
13. Davies, E. V., and Hallett, M. B. (1998) *Int. J. Mol. Med.* **1,** 485–490
14. Partida-Sánchez, S., Cockayne, D. A., Monard, S., Jacobson, E. L., Oppenheimer, N., Garvy, B., Kusser, K., Goodrich, S., Howard, M., Harmsen, A., Randall, T. D., and Lund, F. E. (2001) *Nat. Med.* **7,** 1209–1216
15. Partida-Sánchez, S., Iribarren, P., Moreno-Garcia, M. E., Gao, J. L., Murphy, P. M., Oppenheimer, N., Wang, J. M., and Lund, F. E. (2004) *J. Immunol.* **172,** 1896–1906
16. Communi, D., Govaerts, C., Parmentier, M., and Boeynaems, J. M. (1997) *J. Biol. Chem.* **272,** 31969–31973
17. Qi, A.-D., Kennedy, C., Harden, T. K., and Nicholas, R. (2001) *Br. J. Pharmacol.* **132,** 318–326
18. Torres, B., Zambon, A. C., and Insel, P. A. (2002) *J. Biol. Chem.* **277,** 7761–7765
19. Ullmann, H., Meis, S., Hongwiset, D., Marzian, C., Wiese, M., Nickel, P., Communi, D., Boeynaems, J. M., Wolf, C., Hausmann, R., Schmalzing, G., and Kassack, M. U. (2005) *J. Med. Chem.* **48,** 7040–7048
20. Graeff, R., and Lee, H. C. (2002) *Biochem. J.* **361,** 379–384
21. Bradford, M. (1976) *Anal. Biochem.* **72,** 248–252
22. Walseth, T. F., and Lee, H. C. (1993) *Biochim. Biophys. Acta* **1178,** 235–242
23. Lee, H. C. (2002) in *Cyclic ADP-Ribose and NAADP: Structures, Metabolism and Functions*, Kluwer Academic Publishers, Norwell, MA
24. Di Virgilio, F., Chiozzi, P., Ferrari, D., Falzoni, S., Sanz, J. M., Morelli, A., Torboli, M., Bolognesi, G., and Baricordi, O. R. (2001) *Blood* **97,** 587–600
25. la Sala, A., Ferrari, D., Di Virgilio, F., Idzko, M., Norgauer, J., and Girolomoni, G. (2003) *J. Leukoc. Biol.* **73,** 339–343
26. Ralevic, V., and Burnstock, G. (1998) *Pharmacol. Rev.* **50,** 413–492
27. Merritt, J. E., Armstrong, W. P., Benham, C. D., Hallam, T. J., Jacob, R., Jaxa-Chamiec, A., Leigh, B. K., McCarthy, S. A., Moores, K. E., and Rink, T. J. (1990) *Biochem. J.* **271,** 515–522
28. Lee, H. C., and Aarhus, R. (1991) *Cell Regul.* **2,** 203–209
29. Meshki, J., Tuluc, F., Bredetean, O., Ding, Z., and Kunapuli, S. P. (2004) *Am. J. Physiol.* **286,** C264–C271
30. Ziegler, M. (2000) *Eur. J. Biochem.* **267,** 1551–1564
31. Dubyak, G. R., and Cowen, D. S. (1990) *Ann. N. Y. Acad. Sci.* **603,** 227–244
32. Beigi, R. D., Kertesy, S. B., Aquilina, G., and Dubyak, G. R. (2003) *Br. J. Pharmacol.* **140,** 507–519
33. White, P. J., Webb, T. E., and Boarder, M. R. (2003) *Mol. Pharmacol.* **63,** 1356–1363
34. Spassova, M. A., Soboloff, J., He, L. P., Hewavitharana, T., Xu, W., Venkatachalam, K., van Rossum, D. B., Patterson, R. L., and Gill, D. L. (2004) *Biochim. Biophys. Acta* **1742,** 9–20
35. Kiselyov, K., Shin, D. M., Shcheynikov, N., Kurosaki, T., and Muallem, S. (2001) *Biochem. J.* **360,** 17–22
36. Rah, S. Y., Park, K. H., Han, M. K., Im, M. J., and Kim, U. H. (2005) *J. Biol. Chem.* **280,** 2888–2895
37. Schwarzmann, N., Kunerth, S., Weber, K., Mayr, G. W., and Guse, A. H. (2002) *J. Biol. Chem.* **277,** 50636–50642
38. Guse, A. H. (2005) *FEBS J.* **272,** 4590–4597
39. Gasser, A., Glassmeier, G., Fliegert, R., Langhorst, M. F., Meinke, S., Hein, D., Kruger, S., Weber, K., Heiner, I., Oppenheimer, N., Schwarz, J. R., and Guse, A. H. (2006) *J. Biol. Chem.* **281,** 2489–2496
40. Kolisek, M., Beck, A., Fleig, A., and Penner, R. (2005) *Mol. Cell* **18,** 61–69
41. Bruzzone, S., Guida, L., Zocchi, E., Franco, L., and De Flora, A. (2001) *FASEB J.* **15,** 10–12
42. Smyth, L. M., Bobalova, J., Mendoza, M. G., Lew, C., and Mutafova-Yambolieva, V. N. (2004) *J. Biol. Chem.* **279,** 48893–48903
43. Bruzzone, S., Franco, L., Guida, L., Zocchi, E., Contini, P., Bisso, A., Usai, C., and De Flora, A. (2001) *J. Biol. Chem.* **276,** 48300–48308